Dynamics and Energetics of Ge(001) Dimers

Arie van Houselt, Raoul van Gastel, Bene Poelsema, and Harold J. W. Zandvliet

Physical Aspects of Nanoelectronics and Solid State Physics, MESA$^+$ Institute for Nanotechnology, University of Twente, P.O. Box 217, 7500 AE Enschede, The Netherlands

(Received 15 August 2006; published 28 December 2006)

The dynamic behavior of surface dimers on Ge(001) has been studied by positioning the tip of a scanning tunneling microscope over single flip-flopping dimers and measuring the tunneling current as a function of time. We observe that not just symmetric, but also asymmetric appearing dimers exhibit flip-flop motion. The dynamics of flip-flopping dimers can be used to sensitively gauge the local potential landscape of the surface. Through a spatial and time-resolved measurement of the flip-flop frequency of the dimers, local strain fields near surface defects can be accurately probed.

DOI: 10.1103/PhysRevLett.97.266104 PACS numbers: 68.35.Dv, 68.35.Bs, 68.37.Ef

The silicon and germanium semiconductor group IV (001) surfaces are among the most frequently studied surfaces in literature [1–3]. Because of its obvious technological importance to the semiconductor industry, the majority of studies have, however, been devoted to the Si(001) surface rather than the closely related Ge(001) surface. Both (001) surfaces are examples of a system that exhibits both a strong short-range interaction and a weak long-range interaction. The short-range interaction leads to dimerization, i.e., a pairing of nearest-neighbor surface atoms to form a (2×1) reconstruction [4]. The weaker long-range interaction results in various higher-order surface reconstructions, such as $p(2 \times 2)$ and $c(4 \times 2)$. In several other aspects the Ge(001) surface [2] also turns out to be very similar to the Si(001) surface [3]. The properties and possible applications resulting from the dimerized termination of both surfaces has been the topic of many recent papers, investigating, e.g., the formation of heteroepitaxial nanostructures, the chemical reactivity of the bare (001) surfaces and the application of both surfaces in high-efficiency solar cells [5–8].

In 1985 the first scanning tunneling microscopy (STM) images of the Si(001) surface [9,10] revealed that most of the surface dimers have a symmetric appearance. However, it has been well established since than that the lowest energy configuration is a buckled dimer [11,12]. The observed symmetric dimers are actually flip flopping rapidly between the two possible buckled configurations [13–16]. The first direct evidence for this flip-flop motion was provided by Sato, Iwatsuki, and Tochihara [13]. They demonstrated that the tunneling current recorded above one of the atoms of a dimer of the Ge(001) surface exhibited telegraph like noise. A few years later similar experiments were reported for Si(001) by Hata *et al.* [14], Yoshida *et al.* [15], and Pennec *et al.* [16]. The latter measurements demonstrated that the flip-flop motion of the dimers can be interpreted in terms of a so-called phason. A phason is a phase defect in the dimer alignment. At sufficiently high temperatures phasons perform a thermally activated (biased) random walk. A dimer, which is positioned under an STM tip is flipped and the tunneling resistance is changed, each time a phason traverses the tunnel junction.

In this Letter we investigate the thermal motion of flip-flopping dimers in the different reconstructions that occur on the Ge(001) surface. The motion of the dimers is monitored by recording the telegraph noise in the tunneling current of an STM tip, when it is positioned directly over a dimer. By performing these measurements in a spatially resolved manner in the vicinity of specific surface defects, we are able to directly and sensitively probe the effect of such features on the energetics and dynamics of the dimers.

The experiments were performed in an ultrahigh vacuum (UHV) system, equipped with a room temperature Omicron STM and a base pressure of 3×10^{-11} mbar. After degassing the nearly intrinsic Ge(001) samples at 900 K, they were further cleaned by cycles of Ar^+ bombardment (800 eV, 2 μA/cm^2, angle of incidence 45°, 20 min) and annealing at 1100 K for a few minutes. During annealing the pressure in the vacuum system did not rise above 3×10^{-10} mbar. This procedure resulted in an atomically clean Ge(001) surface that exhibited ordered $(2 \times 1)/c(4 \times 2)$ domain patterns [17] with a low concentration ($\approx 0.001\%$ of a monolayer) of missing dimer defects. After equilibration to room temperature the sample was placed in the STM for observation.

Figure 1(a) shows a room temperature STM image of the Ge(001) surface. The surface shows an ordered $c(4 \times 2)/(2 \times 1)$ domain pattern [17]. Within a single substrate dimer row the dimers buckle nearly always in an antiferromagnetic order, meaning that neighboring dimers buckle in opposite directions. The antiferromagnetic order partially relaxes the stress generated by the buckling of the dimers. In-phase buckling of adjacent dimer rows leads to a $p(2 \times 2)$ reconstruction, whereas out-of-phase buckling of adjacent dimer rows leads to a $c(4 \times 2)$ reconstruction [3]. In the two latter cases, the asymmetric appearance of the dimers is generally perceived to imply that the flip-flop motion is frozen in.

We have performed room temperature measurements of the flip-flop motion of dimers ordered in (2×1) and $c(4 \times 2)$ domains, as shown in Fig. 1(b). Symmetric appearing

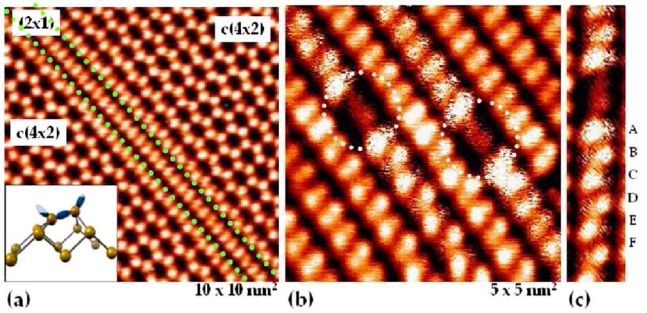

FIG. 1 (color online). (a) Filled-state room temperature STM image of Ge(001). The sample bias is −1.5 V, and the tunneling current is 0.4 nA. The local $c(4 \times 2)$ and (2×1) reconstructions are indicated. At the phase boundary between the 2 domains, green dotted lines have been added as a guide to the eye. Note that the domain boundary has a finite width that shows up as a reduced buckling amplitude in dimer rows directly adjacent to the domain boundary. Inset: Schematic representation of a buckled dimer. The tilt angle of the dimer is about 10°–20°. (b) Filled-state STM image of Ge(001) ($V_{\text{bias}} = -1.5$ V, $I_{\text{tunnel}} = 0.4$ nA). The flickering in some of the substrate dimer rows is due to the flip-flop motion of dimers during imaging. The flickering occurs in rows that contain a missing dimer defect. Note that this flickering occurs both in a symmetric dimer row (right defect) and an asymmetric dimer row (left defect). (c) The dimer positions where the current is measured as a function of time are labeled A–F.

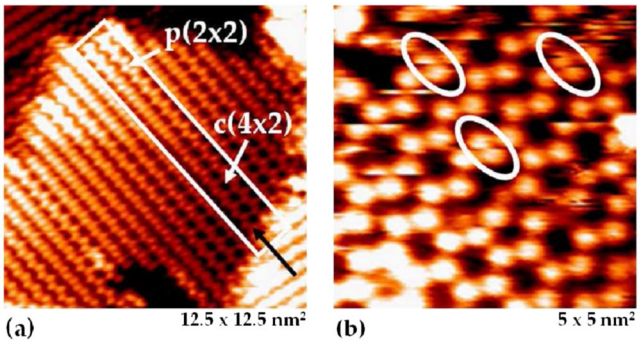

FIG. 2 (color online). (a) A phason trapped between two steps. The image is recorded at 300 K. The sample bias is −1.5 V and the tunneling current is 0.5 nA. Two dimer rows are highlighted by a white box. The gradual change from a $c(4 \times 2)$ to a $p(2 \times 2)$ registry (white arrows) in the lower of the two dimer rows, pointed to by the black arrow, indicates the presence of a rapidly diffusing phason in this row. (b) STM image of the Ge(001) surface recorded at 77 K. During imaging, diffusing phasons pass through the imaged dimer rows. This gives rise to double lobed dimers, marked by the white ellipses. Although it is tempting to interpret the streakiness in some of the scan lines in terms of tip changes, all apparent discontinuities in the imaged dimers can be explained in terms of these diffusion events. They show up as discontinuities only in small segments of a scan line rather than in an entire line. The sample bias is −1.5 V and the tunneling current is 0.4 nA.

dimers are visible in the lower-left and upper-right corners of the image. In the middle of the image two missing dimer defects are visible (dotted white circles). The missing dimer defect on the left induces buckling of the nearby dimers, whereas the right one results in symmetric appearing dimers. The dimer rows that contain the missing dimer defects both have a noisy appearance, indicative of a rapid flip-flopping motion of the dimers. Interestingly, the flickering is not only observed in the dimer row that appears symmetric, but also in the one that appears asymmetric. This observation conflicts directly with the picture of static buckled dimers in the $c(4 \times 2)$ phase. It should be pointed out that there are also buckled dimers that do not show any telegraph noise, at least not on the time scale that is accessible to our instrument. Their motion is either too slow or too fast for us to observe (sampling time during imaging is around 1 ms per pixel).

The flip-flop motion of the dimers is a consequence of the presence of phase defects in the antiferromagnetic dimer alignment (phasons). The dimer under the tip is flipped each time a phason makes an in-plane traversal of the tip surface junction.

Figure 2 shows two examples of phasons on the Ge(001) surface. In Fig. 2(a) a room temperature image of a phason trapped between two step edges is depicted. Figure 2(b) shows diffusing phasons at 77 K. Because of the diffusion of the phason during imaging the highlighted dimers appear as double lobed features.

To investigate the dynamics of the dimer flip-flop motion in more detail, the tunneling current is measured at room temperature as a function of time at various dimer sites, labeled A–F in Fig. 1(c). To correct for the attractive interaction between tip and diffusing phasons, described by Pennec *et al.* [16], the tunneling current is measured over each pixel of the STM picture. The width of one dimer is approximately 40 pixels in our STM images. The telegraph noise of one dimer is thus sampled many times using various tunneling resistances. In this way the variation in the lateral distance between the tip and the dimer allows us to verify and exclude the presence of significant interactions between the tip and the switching dimer.

Figure 3(a) shows a typical current trace measured above a flickering asymmetric dimer [curve (1)], above a flickering symmetric dimer [curve (2)], above a nonflickering symmetric dimer [curve (3)] and above a nonflickering asymmetric dimer [curve (4)]. From the telegraph noise it is obvious that the flickering asymmetric dimer has a preference for one of the buckled states, whereas the flickering symmetric dimer does not exhibit such a preference. It is most likely that the flip-flop frequency of the nonflickering symmetric and asymmetric dimers is so high that it lies outside the bandwidth of the STM preamplifier (≈ 40 kHz). The distribution of the residence times of the dimers in each of the two buckled states was measured and is shown in a histogram $H(t)$ for the flickering symmetric dimers in Fig. 3(b) and for the flickering asymmetric

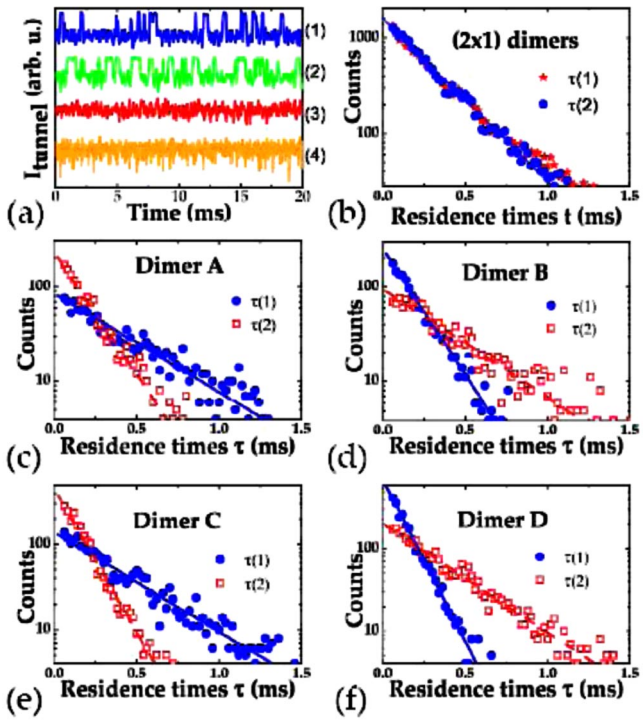

FIG. 3 (color online). (a) Current traces measured on a flickering asymmetric dimer [curve (1)], a flickering symmetric dimer [curve (2)], a nonflickering symmetric dimer [curve (3)], and a nonflickering asymmetric dimer [curve (4)]. The sampling rate is 50 kHz and the total sampling time is 20–80 ms. (b) Histogram of the residence times in the two buckled states of a symmetric appearing dimer. The line is the theoretical fit for a random process (Poission distribution). $\tau(1)$ and $\tau(2)$ are the counts for the two residence times in the two different states. (c–f) Histograms of the residence times for dimers A–D from Fig. 1(c). The lines are the corresponding theoretical curves for a random process. $\tau(1)$ and $\tau(2)$ are the counts for the two residence times in the two different states.

dimers in Figs. 3(c)–3(f). Assuming that the flip-flop motion is a random process, the theoretical lines are obtained from the following relation,

$$H(t) = \frac{N}{2} p_{ij}(1 - p_{ij})^t, \tag{1}$$

where p_{ij} is the probability to flip from state (i) to state (j), N is the number of flip-flop events and t is the time. The factor $N/2$ results from the fact that half of the flip-flop events are from state (i) to state (j) and the other half from state (j) to state (i). N and p_{ij} are determined from the distribution of the residence times. All histograms of the measured residence times in Figs. 3(b)–3(f) show Poisson behavior. The average residence times in the two configurations of the symmetric dimer are about the same, whereas they are significantly different for the asymmetric appearing dimers labeled A–D. As a function of distance from the defect, via dimer A–F, the dimers show an alternating preference for either state (1) (dimers A, C, E, etc.) or state (2) (dimers B, D, F, etc.), in accordance with the observed $c(4 \times 2)$ (zigzag) reconstruction. State (1) here means a dimer is buckled such that the "left" atom is higher; see Fig. 1(c), state (2) means the "right" atom is higher. The difference in average residence times of the asymmetric appearing dimers allows us to determine the energy difference for the two buckled configurations, using

$$\frac{\langle\tau(1)\rangle}{\langle\tau(2)\rangle} = \exp\frac{\Delta E}{k_B T}, \tag{2}$$

where k_B is Boltzmann's constant and T is temperature. The energy difference between the buckled dimers labeled A–F is 22 ± 2 meV.

Next, we investigate the spatial variation of the flip-flop frequency of dimers near defects to probe the interaction between the phason and the defect. We define the flip-flop frequency of a dimer as the inverse of the average time between successive passages of a phason ($\frac{1}{\langle\tau(1)\rangle+\langle\tau(2)\rangle}$). In Fig. 4 the flip-flop frequency of several dimers is plotted as a function of distance to the missing dimer defect. For both the symmetric and asymmetric dimer row the frequency just near the missing dimer defect is ≈ 3 kHz and it gradually increases away from the defect. The increase in flip-flop frequency of the asymmetric dimers with increasing distance from the defect confirms our suspicion that the flip-flop motion of nonflickering asymmetric dimers at room temperature is indeed outside the available bandwidth of our setup. The decrease of the flip-flop frequency near the defect effectively constitutes a repulsive interaction between the missing dimer defect and the diffusing phason. By analyzing the spatial variations of the flip-flop frequency, the exact distance dependence of the repulsive interaction between the defect and the phason can be extracted in a straightforward manner. Considering two dimer positions, one just adjacent to the missing dimer defect (ν_0) and the other further away in the dimer row (ν_i), the interaction energy between these two dimers is determined by $\nu_i = \nu_0 \exp\frac{-\Delta E_i}{k_B T}$. In Fig. 5 the interaction energies ΔE are plotted versus the distance Δx from the dimer next to the defect. To interpret the magnitude of the interaction energies, we need to realize that the introduction of both defects on the surface implies an interruption

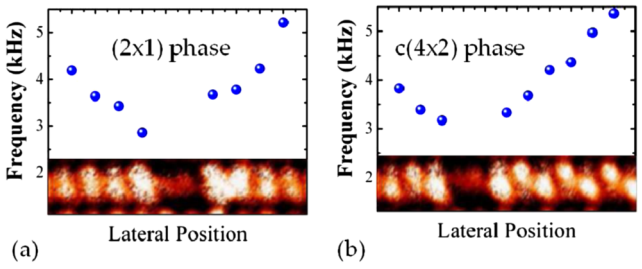

FIG. 4 (color online). Flip-flop frequency as a function of the lateral position from a missing dimer defect for symmetric dimers (a) and for asymmetric dimers (b).

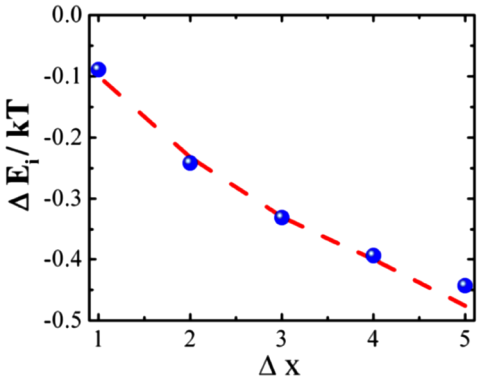

FIG. 5 (color online). The repulsive interaction as extracted from the spatial dependence of the flip-flop frequency versus the position. The solid line refers to a logarithmically decaying repulsive interaction following Eq. (3). The data shown is for the $c(4 \times 2)$ dimers.

of the regular dimerized surface termination. This in turn leads to the creation of strain fields associated with each of the defects. We thus propose that the repulsion between the missing dimer defect and the phason is the result of long-ranged elastic interaction between the particles. The interaction energy (strain relaxation energy per surface lattice constant) in terms of surface stress anisotropy, $\Delta\sigma$ between them is given by [18,19]:

$$E(\Delta x) = -\frac{(1-\nu)}{2\pi\mu}(\Delta\sigma)^2 \ln\left(\frac{\Delta x}{\pi a_c}\right), \qquad (3)$$

where ν and μ are the Poisson ratio and the bulk modulus of Ge, respectively, ($\frac{(1-\nu)}{2\pi\mu} \approx 0.01$ a^3/eV) and a_c is the microscopic cutoff length. Using Eq. (3), we have fitted our data, as depicted in Fig. 5. The value that we find for the surface stress anisotropy, $\Delta\sigma$, is ≈ 0.5 eV/a^2 (0.5 N/m). An identical value is obtained for the (2×1) phase. This value should be compared with the surface stress along the dimer row direction of the Ge(001) surface. For the closely related Si(001) surface, values of the surface stress along the dimer row direction of the different higher-order reconstructions are reported in the range of 0.5–2 eV/a^2 [20,21].

We have studied the flip-flop motion of dimers on the Ge(001) surface. We have shown that both symmetric and asymmetric dimers exhibit flip-flop motion at room temperature. The flip-flop motion of the dimers is a direct result of the diffusion of phase defects, aka, phasons, along the substrate dimer rows. The interaction of phasons with missing dimer defects was studied by measuring flip-flop frequencies in the vicinity of such defects. We found a strain relaxation driven, logarithmically decaying, repulsive interaction between the diffusing phase defects and missing dimer defects. The identical elastic properties of the (2×1) and $c(4 \times 2)$ rows also hint that the basic atomic configuration of the two phases is essentially identical, the only difference being in the energies of each of the two buckled states. The flip-flop frequency of Ge(001) dimers in turn can be used as a probe for the potential landscape of the surface.

This work is financially supported by the Stichting voor Fundamenteel Onderzoek der Materie (FOM, 03PR2208).

[1] J. Dąbrowski and H.-J. Müssig, *Silicon Surfaces and Formation of Interfaces* (World Scientific, River Edge, NJ, 2000).
[2] H. J. W. Zandvliet, Phys. Rep. **388**, 1 (2003).
[3] H. J. W. Zandvliet, Rev. Mod. Phys. **72**, 593 (2000).
[4] R. E. Schlier and H. E. Farnsworth, J. Chem. Phys. **30**, 917 (1959).
[5] O. Gürlü, O. A. O. Adam, H. J. W. Zandvliet, and B. Poelsema, Appl. Phys. Lett. **83**, 4610 (2003).
[6] E. J. Buehler and J. J. Boland, Science **290**, 506 (2000).
[7] P. W. Loscutoff and S. F. Bent, Annu. Rev. Phys. Chem. **57**, 467 (2006).
[8] S. Gan *et al.*, J. Appl. Phys. **85**, 2004 (1999).
[9] R. M. Tromp, R. J. Hamers, and J. E. Demuth, Phys. Rev. Lett. **55**, 1303 (1985).
[10] R. J. Hamers, R. M. Tromp, and J. E. Demuth, Phys. Rev. B **34**, 5343 (1986).
[11] D. J. Chadi, Phys. Rev. Lett. **43**, 43 (1979).
[12] Y. J. Li, H. Nomura, N. Ozaki, Y. Naitoh, M. Kageshima, Y. Sugawara, C. Hobbs, and L. Kantorovich, Phys. Rev. Lett. **96**, 106104 (2006).
[13] T. Sato, M. Iwatsuki, and H. Tochihara, J. Electron Microsc. **48**, 1 (1999).
[14] K. Hata, Y. Sainoo, and H. Shigekawa, Phys. Rev. Lett. **86**, 3084 (2001).
[15] S. Yoshida, O. Takeuchi, K. Hata, R. Morita, M. Yamashita, and H. Shigekawa, Jpn. J. Appl. Phys. **41**, 5017 (2002).
[16] Y. Pennec, M. Horn von Hoegen, Xiaobin Zhu, D. C. Fortin, and M. R. Freeman, Phys. Rev. Lett. **96**, 026102 (2006).
[17] H. J. W. Zandvliet, B. S. Swartzentruber, W. Wulfhekel, B. J. Hattink, and B. Poelsema, Phys. Rev. B **57**, R6803 (1998).
[18] V. I. Marchenko, Pis'ma Zh. Eksp. Teor. Fiz. **33**, 397 (1981) [JETP Lett. **33**, 381 (1981)].
[19] O. L. Alerhand, D. Vanderbilt, R. D. Meade, and J. D. Joannopoulos, Phys. Rev. Lett. **61**, 1973 (1988).
[20] A. García and J. E. Northrup, Phys. Rev. B **48**, 17 350 (1993).
[21] J. Dąbrowski, E. Pehlke, and M. Scheffler, Phys. Rev. B **49**, 4790 (1994).